Onset of Convection in a Porous Rectangular Channel with External Heat Transfer to Upper and Lower Fluid Environments

A. Barletta · L. Storesletten

Abstract The conditions for the onset of convection in a horizontal rectangular channel filled with a fluid saturated porous medium are studied. The vertical sidewalls are assumed to be impermeable and adiabatic. The horizontal upper and lower boundary walls are considered as impermeable and subject to external heat transfer, modelled through a third-kind boundary condition on the temperature field. The external fluid environments above and below the channel, kept at different temperatures, provide the heating-from-below mechanism which may lead to the onset of the thermal instability in the porous medium. The linear response of the fluid saturated porous channel, in a basic motionless state, is tested with respect to three-dimensional normal mode disturbances of the temperature field and of the pressure field. The linearised disturbance equations are solved analytically leading to an implicit-form expression of the neutral stability condition, formulated as a functional relationship between the Darcy–Rayleigh number and the continuous longitudinal wave number of the normal modes, for any assigned aspect ratio of the cross-section and for any given Biot number. The analysis of the neutral stability is carried out. The analysis is extended to the case of a channel with a finite length in the longitudinal direction, and with adiabatic and impermeable capped ends.

Keywords Rectangular porous channel · Darcy's law · Linear stability · Darcy–Bénard problem · Third-kind temperature conditions · Analytical solution

1 Introduction

The thermal instability of porous layers of finite or infinite width, subject to heating-from-below, is a classical topic of growing interest for the heat transfer community. In the recent

A. Barletta (✉)
DIENCA, Alma Mater Studiorum-Università di Bologna, Viale Risorgimento 2, 40136 Bologna, Italy
e-mail: antonio.barletta@unibo.it

L. Storesletten
Department of Mathematics, University of Agder, Postboks 422, 4604 Kristiansand, Norway
e-mail: leiv.storesletten@uia.no

decades, several new results have been achieved on this subject surveyed, for instance, by Rees (2000), Tyvand (2002), Nield and Bejan (2006) and Barletta (2011). In particular, recent studies have shown the role played by temperature boundary conditions of the third kind, describing a wall heat transfer regime intermediate between the first kind (Dirichlet-type) temperature conditions, and the second kind (Neumann-type) temperature conditions. To the best of our knowledge, the studies on the effect of third-kind temperature conditions, prescribed at the sidewalls of a vertical layer, on the thermal instability in a porous medium were initiated by Weidman and Kassoy (1986). More recently, Kubitschek and Weidman (2003) analysed the thermal instability in a fluid saturated porous box where the lower horizontal boundary is heated through an external forced convection process, parametrised by a Biot number, while the upper horizontal boundary is maintained isothermal. The Biot number is, in fact, the dimensionless parameter involved when third-kind temperature conditions are used to model the boundary heat transfer (see, for instance, Incropera et al. 2011). We mention that Nygård and Tyvand (2010, 2011), on studying the thermal instability in a porous box (Nygård and Tyvand 2010), and in a vertical porous cylinder (Nygård and Tyvand 2011), considered third-kind boundary conditions for the temperature field in the case of partially permeable boundary walls. Mojtabi and Rees (2011), as well as Rees and Mojtabi (2011), obtained third-kind boundary conditions for the temperature disturbances in the stability analysis of a saturated porous layer bounded by walls with a finite and non-negligible thermal conductance. A peculiar feature in this case is that the Biot number depends on the wave number of the disturbance. Barletta and Storesletten (2011) studied the onset of the thermal instability in a circular porous duct saturated by a fluid and subject to a temperature boundary condition of the third kind.

In a recent paper (Barletta and Storesletten 2012), the onset of the thermal instability in a horizontal channel with a rectangular cross-section has been investigated by assuming an infinite longitudinal length of the channel and a motionless rest state. In this study, the vertical impermeable sidewalls were assumed to be subject to an external convection process, modelled by temperature boundary conditions of the third kind. The role of the Biot number in determining the onset conditions of the instability was described. The assumption of an infinite channel length was finally relaxed in order to establish the behaviour in the case of a discrete spectrum for the longitudinal wave number of the normal modes employed in the linear stability analysis.

The aim of the present contribution, is to continue the investigation carried out in Barletta and Storesletten (2012), by testing the effect of the third-kind temperature conditions applied on the horizontal boundary walls (upper and lower) of a rectangular porous channel. This study is also related to that reported by Kubitschek and Weidman (2003), with the substantial difference that Kubitschek and Weidman (2003) assumed an isothermal upper boundary. Thus, in the limiting case of an infinite Biot number, Kubitschek and Weidman (2003) found the condition of isoflux/isothermal horizontal boundaries leading to a value 27.096 for the critical Darcy–Rayleigh number at the onset of convection (Ribando and Torrance 1976; Wang 1999). On the other hand, in the limiting case of an infinite Biot number, this study will lead to a value 12 corresponding to the case where both the horizontal boundaries are impermeable and isoflux (Nield 1968; Nield and Bejan 2006). The study of the linear stability will be developed on assuming different values of the Biot number and of the cross-sectional aspect ratio. Then, the critical values of the Darcy–Rayleigh number will be determined and shown to be independent of the aspect ratio, while they display a monotonic increasing dependence on the Biot number. Finally, the assumption of an infinite longitudinal length will be released, in analogy with the analysis reported in Barletta and Storesletten (2012),

so that the longitudinal wave number of the normal mode disturbances displays a discrete spectrum.

2 Mathematical Model

We consider natural convection in a horizontal channel filled with a fluid saturated porous medium. The channel is rectangular with height H and width $2L$, and we choose a Cartesian coordinate system with the $\bar{y}$-axis in the vertical direction and the $\bar{x}$-axis in the horizontal direction perpendicular to the channel sidewalls. The horizontal channel walls are at $\bar{y} = 0$ and $\bar{y} = H$, and the vertical walls at $\bar{x} = -L$ and $\bar{x} = L$; see Fig. 1. Relative to the Cartesian set of coordinates $(\bar{x}, \bar{y}, \bar{z})$, the components of the seepage velocity $\bar{\mathbf{u}}$ are denoted as $(\bar{u}, \bar{v}, \bar{w})$, respectively. We assume that the effect of viscous dissipation is negligible and that the solid and fluid phases are in local thermal equilibrium. We also consider as negligible the effects of a possible heterogeneity in the porous medium (the thermal instability in heterogeneous porous media has been recently studied, for instance, by Barletta et al. 2011, 2012). Then, according to the Oberbeck–Boussinesq approximation, the local balance equations for mass, momentum and energy can be written as

$$\bar{\nabla} \cdot \bar{\mathbf{u}} = 0, \tag{1a}$$

$$\frac{\mu}{K} \bar{\mathbf{u}} = -\bar{\nabla} \bar{p} + \rho g \beta \left(\bar{T} - T_0 \right) \hat{\mathbf{e}}_y, \tag{1b}$$

$$\sigma \frac{\partial \bar{T}}{\partial \bar{t}} + \bar{\mathbf{u}} \cdot \bar{\nabla} \bar{T} = \alpha \bar{\nabla}^2 \bar{T}. \tag{1c}$$

Here, $\bar{p}$ is the difference between the pressure and the hydrostatic pressure, μ is the dynamic viscosity of the fluid, K is the permeability, ρ is the fluid density, β is the thermal expansion coefficient, $\hat{\mathbf{e}}_y$ is the unit vector along the vertical $\bar{y}$-axis, $\mathbf{g} = -g\,\hat{\mathbf{e}}_y$ is the gravitational acceleration with modulus g, $\bar{T}$ is the temperature field and T_0 is the reference temperature, $\bar{t}$ is the time, α is the average thermal diffusivity and σ is the ratio between the average volumetric heat capacity of the fluid saturated porous medium and the volumetric heat capacity of the fluid.

The channel walls are assumed to be impermeable. The lateral boundary walls at $\bar{x} = \pm L$ are adiabatic, while heat transfer to the external fluid environments occurs through the horizontal boundary walls. The lower boundary wall, $\bar{y} = 0$, exchanges heat by convection with an underlying fluid such that the temperature of the outer flow is $T_0 + \Delta T/2$, with $\Delta T > 0$. The upper boundary wall, $\bar{y} = H$, exchanges heat by convection with an external fluid such that the temperature of the outer flow is $T_0 - \Delta T/2$. We assume the same external heat transfer coefficient, h, both at the lower boundary and at the upper boundary. The boundary conditions then become

$$\bar{y} = 0, \quad -L < \bar{x} < L : \bar{v} = 0, \quad k \frac{\partial \bar{T}}{\partial \bar{y}} = h \left(\bar{T} - T_0 - \frac{\Delta T}{2} \right), \tag{2a}$$

$$\bar{y} = H, \quad -L < \bar{x} < L : \bar{v} = 0, \quad -k \frac{\partial \bar{T}}{\partial \bar{y}} = h \left(\bar{T} - T_0 + \frac{\Delta T}{2} \right), \tag{2b}$$

$$\bar{x} = \pm L, \quad 0 < \bar{y} < H : \bar{u} = 0, \quad \frac{\partial \bar{T}}{\partial \bar{x}} = 0. \tag{2c}$$

The boundary conditions, Eqs. (2a) and (2b), for the temperature field in the porous medium are third-kind, or Robin, boundary conditions and they are just a consequence of Newton's
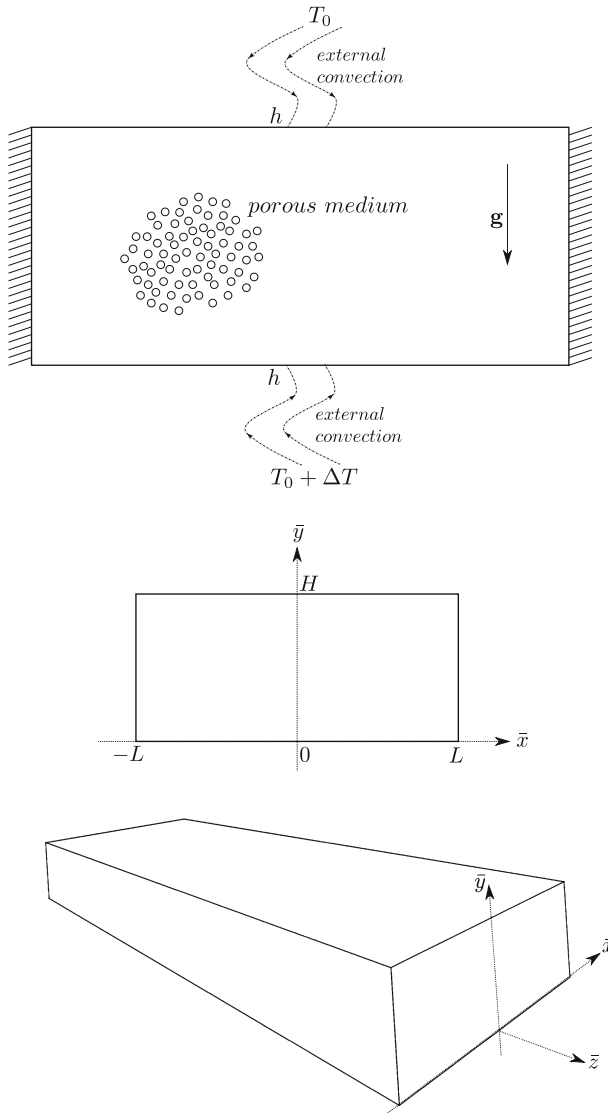
Fig. 1 Sketch of the rectangular porous channel

cooling law. This law models the boundary heat transfer from a body to the environment, whenever the heat transfer means convection to an external fluid.

2.1 Dimensionless Equations

The dimensional fields, coordinates, time and nabla operator are denoted by an overline. The corresponding dimensionless quantities are defined as

$$(\bar{x}, \bar{y}, \bar{z}) = (x, y, z)H, \quad (\bar{u}, \bar{v}, \bar{w}) = (u, v, w)\,\frac{\alpha}{H}, \quad \bar{\nabla} = \frac{1}{H}\,\nabla,$$

$$\bar{T} = T_0 + T\,\Delta T, \quad \bar{p} = p\,\frac{\mu\alpha}{K}, \quad \bar{t} = t\,\frac{\sigma H^2}{\alpha}. \tag{3}$$

The governing equations (1) and (2) can be rewritten in a dimensionless form as:

$$\nabla \cdot \mathbf{u} = 0, \tag{4a}$$

$$\mathbf{u} = -\nabla p + R\,T\,\hat{\mathbf{e}}_y, \tag{4b}$$

$$\frac{\partial T}{\partial t} + \mathbf{u} \cdot \nabla T = \nabla^2 T, \tag{4c}$$

where the Darcy–Rayleigh number R, the Biot number B and the aspect ratio s are given by

$$R = \frac{\rho g \beta K H \Delta T}{\mu \alpha}, \quad B = \frac{hH}{k}, \quad s = \frac{L}{H}. \tag{5}$$

The boundary conditions (2) can be rewritten as

$$y = 0, \quad -s < x < s : v = 0, \quad \frac{\partial T}{\partial y} = B\left(T - \frac{1}{2}\right), \tag{6a}$$

$$y = 1, \quad -s < x < s : v = 0, \quad \frac{\partial T}{\partial y} = -B\left(T + \frac{1}{2}\right), \tag{6b}$$

$$x = \pm s, \quad 0 < y < 1 : u = 0, \quad \frac{\partial T}{\partial x} = 0. \tag{6c}$$

The limiting cases $B \to \infty$ and $B \to 0$ correspond to isothermal horizontal boundaries and to thermally insulated (adiabatic) horizontal boundaries, respectively.

2.2 Basic Solution

There exists a stationary solution of Eqs. (4) and (6) given by

$$u_b = v_b = w_b = 0, \quad T_b = -\frac{B}{B+2}\left(y - \frac{1}{2}\right),$$

$$p_b = p_0 + \frac{RB}{2(B+2)}\left(y - y^2\right), \tag{7}$$

where "b" stands for "basic solution", and p_0 is an arbitrary integration constant.

3 Linear Disturbances

Let us first eliminate the velocity components (u, v, w) by substituting Eq. (4b) into Eqs. (4a) and (4c), which yields

$$\nabla^2 p = R\,\frac{\partial T}{\partial y}, \tag{8a}$$

$$\frac{\partial T}{\partial t} - \nabla p \cdot \nabla T + RT\,\frac{\partial T}{\partial y} = \nabla^2 T. \tag{8b}$$

The boundary conditions are

$$y = 0, \quad -s < x < s : \frac{\partial p}{\partial y} = RT, \quad \frac{\partial T}{\partial y} = B\left(T - \frac{1}{2}\right), \tag{9a}$$

$$y = 1, \quad -s < x < s : \frac{\partial p}{\partial y} = RT, \quad \frac{\partial T}{\partial y} = -B\left(T + \frac{1}{2}\right), \tag{9b}$$

$$x = \pm s, \quad 0 < y < 1 : \frac{\partial p}{\partial x} = 0, \quad \frac{\partial T}{\partial x} = 0. \tag{9c}$$

We perturb the basic solution, Eq. (7), with small-amplitude disturbances defined by

$$p = p_b + \varepsilon P, \quad T = T_b + \varepsilon \theta, \tag{10}$$

where ε is a small perturbation parameter, while P and θ are the dimensionless pressure and temperature disturbances, respectively.

Following the usual linear stability analysis, we substitute Eq. (10) into Eqs. (8) and (9), and we neglect the terms of order ε^2. Thus, we obtain the governing equations for the disturbances

$$\nabla^2 P = R\frac{\partial \theta}{\partial y}, \tag{11a}$$

$$\nabla^2 \theta = \frac{\partial \theta}{\partial t} + \frac{B}{B+2}\left(\frac{\partial P}{\partial y} - R\theta\right), \tag{11b}$$

subject to the boundary conditions

$$y = 0, \quad -s < x < s : \frac{\partial P}{\partial y} = R\theta, \quad \frac{\partial \theta}{\partial y} = B\theta, \tag{12a}$$

$$y = 1, \quad -s < x < s : \frac{\partial P}{\partial y} = R\theta, \quad \frac{\partial \theta}{\partial y} = -B\theta, \tag{12b}$$

$$x = \pm s, \quad 0 < y < 1 : \frac{\partial P}{\partial x} = 0, \quad \frac{\partial \theta}{\partial x} = 0. \tag{12c}$$

4 Normal Modes

For the analysis of the neutral stability, we are interested in the time-independent solutions of Eqs. (11) and (12). Following the usual normal mode decomposition, we write

$$P(x, y, z) = F_n(y)\cos\left[\frac{n\pi}{2s}(x+s)\right]\cos(az),$$

$$\theta(x, y, z) = G_n(y)\cos\left[\frac{n\pi}{2s}(x+s)\right]\cos(az), \quad n = 0, 1, 2, \ldots. \tag{13}$$

where a is the dimensionless wave number in the horizontal z-direction. We substitute Eq. (13) into Eqs. (11) and (12) so that we obtain

$$\frac{d^2 F_n}{dy^2} - \left[a^2 + \left(\frac{n\pi}{2s}\right)^2\right]F_n - R\frac{dG_n}{dy} = 0, \tag{14a}$$

$$\frac{d^2 G_n}{dy^2} - \left[a^2 + \left(\frac{n\pi}{2s}\right)^2\right]G_n + \frac{B}{B+2}\left(RG_n - \frac{dF_n}{dy}\right) = 0, \tag{14b}$$

with the boundary conditions

$$y = 0 : \frac{\mathrm{d}F_n}{\mathrm{d}y} = RG_n, \quad \frac{\mathrm{d}G_n}{\mathrm{d}y} = BG_n, \tag{15a}$$

$$y = 1 : \frac{\mathrm{d}F_n}{\mathrm{d}y} = RG_n, \quad \frac{\mathrm{d}G_n}{\mathrm{d}y} = -BG_n. \tag{15b}$$

Equations (14) and (15) can be rewritten by defining

$$V_n(y) = -\frac{\mathrm{d}F_n(y)}{\mathrm{d}y} + RG_n(y), \tag{16}$$

so that we obtain

$$\frac{\mathrm{d}^2 V_n}{\mathrm{d}y^2} - \left[a^2 + \left(\frac{n\pi}{2s} \right)^2 \right] (V_n - RG_n) = 0, \tag{17a}$$

$$\frac{\mathrm{d}^2 G_n}{\mathrm{d}y^2} - \left[a^2 + \left(\frac{n\pi}{2s} \right)^2 \right] G_n + \frac{B}{B+2} V_n = 0, \tag{17b}$$

subject to the boundary conditions

$$y = 0 : V_n = 0, \quad \frac{\mathrm{d}G_n}{\mathrm{d}y} = BG_n, \tag{18a}$$

$$y = 1 : V_n = 0, \quad \frac{\mathrm{d}G_n}{\mathrm{d}y} = -BG_n. \tag{18b}$$

The boundary value problem, Eqs. (17) and (18), can be written in a n-independent form by defining the modified wave number b, such that

$$b^2 = a^2 + \left(\frac{n\pi}{2s} \right)^2. \tag{19}$$

Then, Eqs. (17) and (18) assume a form where the explicit dependence on n and s is lost. Hence, we can omit the subscript n from the solutions $V_n(y)$ and $G_n(y)$ and write

$$\frac{\mathrm{d}^2 V}{\mathrm{d}y^2} - b^2 (V - RG) = 0, \tag{20a}$$

$$\frac{\mathrm{d}^2 G}{\mathrm{d}y^2} - b^2 G + \frac{B}{B+2} V = 0, \tag{20b}$$

with

$$y = 0 : V = 0, \quad \frac{\mathrm{d}G}{\mathrm{d}y} = BG, \tag{21a}$$

$$y = 1 : V = 0, \quad \frac{\mathrm{d}G}{\mathrm{d}y} = -BG. \tag{21b}$$

4.1 Solution of the Eigenvalue Problem

Equations (20) and (21) can be solved as an eigenvalue problem. We recognise in fact that Eqs. (20) and (21) are homogeneous, so that the solution (V, G) is scale-invariant. The scale can be fixed by prescribing the additional condition

$$G(0) = 1. \tag{22}$$

The general solution of Eqs. (20) can be obtained analytically by employing the usual method of the characteristic equation. We define the quantities

$$\eta = \frac{B}{B+2}, \quad \lambda_1 = \sqrt{b\left(b + \sqrt{\eta R}\right)}, \quad \lambda_2 = \sqrt{b\left(b - \sqrt{\eta R}\right)}. \tag{23}$$

The solution of Eqs. (20) that satisfies the conditions

$$V(0) = V(1) = 0, \quad G(0) = 1, \quad \left.\frac{dG}{dy}\right|_{y=0} - BG(0) = 0 \tag{24}$$

can be expressed as

$$V(y) = c_1 \exp(-\lambda_1 y) + c_2 \exp(\lambda_1 y) + c_3 \exp(-\lambda_2 y) + c_4 \exp(\lambda_2 y),$$

$$G(y) = -\sqrt{\frac{\eta}{b^2 R}} \left[c_1 \exp(-\lambda_1 y) + c_2 \exp(\lambda_1 y) - c_3 \exp(-\lambda_2 y) - c_4 \exp(\lambda_2 y) \right], \tag{25}$$

where the coefficients c_1, c_2, c_3, c_4 are given by

$$c_1 = \sqrt{\frac{b^2 R}{\eta}} \, \frac{\lambda_2(\cosh \lambda_2 - e^{\lambda_1}) + (2B - \lambda_1)\sinh \lambda_2}{4(\lambda_2 \sinh \lambda_1 + \lambda_1 \sinh \lambda_2)},$$

$$c_2 = -\sqrt{\frac{b^2 R}{\eta}} \, \frac{\lambda_2(\cosh \lambda_2 - e^{-\lambda_1}) + (2B + \lambda_1)\sinh \lambda_2}{4(\lambda_2 \sinh \lambda_1 + \lambda_1 \sinh \lambda_2)},$$

$$c_3 = -\sqrt{\frac{b^2 R}{\eta}} \, \frac{\lambda_1(\cosh \lambda_1 - e^{\lambda_2}) + (2B - \lambda_2)\sinh \lambda_1}{4(\lambda_2 \sinh \lambda_1 + \lambda_1 \sinh \lambda_2)},$$

$$c_4 = \sqrt{\frac{b^2 R}{\eta}} \, \frac{\lambda_1(\cosh \lambda_1 - e^{-\lambda_2}) + (2B + \lambda_2)\sinh \lambda_1}{4(\lambda_2 \sinh \lambda_1 + \lambda_1 \sinh \lambda_2)}. \tag{26}$$

We have not yet applied the boundary condition,

$$\left.\frac{dG}{dy}\right|_{y=1} + BG(1) = 0. \tag{27}$$

Equation (27) yields a constraint equation for the neutral stability,

$$(-\lambda_1 + B)e^{-\lambda_1}c_1 + (\lambda_1 + B)e^{\lambda_1}c_2 - (-\lambda_2 + B)e^{-\lambda_2}c_3 - (\lambda_2 + B)e^{\lambda_2}c_4 = 0. \tag{28}$$

On account of Eqs. (23) and (26), Eq. (28) can be rewritten as

$$2B\lambda_2 \cosh \lambda_2 \sinh \lambda_1 + (2B^2 + b^2)\sinh \lambda_1 \sinh \lambda_2 - \lambda_1 \lambda_2$$
$$+ \lambda_1 \cosh \lambda_1 (\lambda_2 \cosh \lambda_2 + 2B \sinh \lambda_2) = 0, \tag{29}$$

provided that $\lambda_1 \neq 0$ and $\lambda_2 \neq 0$. Equation (29) defines the neutral stability curves in the parametric plane (b, R), for every assigned Biot number B. We now emphasise that Eq. (19) can be interpreted as the consequence of a degeneracy in the neutral stability condition. In fact, each neutral stability curve $R(b)$ generates, on applying Eq. (19), infinitely many neutral stability curves $R(a, n)$: one for every assigned s and $n = 0, 1, 2, \ldots$. In particular, if b_c and R_c are the critical values of b and R, corresponding to the absolute minimum of the neutral stability curve $R(b)$ for a given B, one may obtain the corresponding critical wave numbers a_c for a prescribed aspect ratio s, as

$$a_c = \sqrt{b_c^2 - \left(\frac{n\pi}{2s}\right)^2}, \tag{30}$$

With $b_c > 0$, then we have $a_c > 0$ if n is such that

$$b_c^2 - \left(\frac{n\pi}{2s}\right)^2 > 0, \tag{31}$$

and $a_c = 0$ if n is such that

$$b_c^2 - \left(\frac{n\pi}{2s}\right)^2 = 0. \tag{32}$$

One may also have n-modes where the expression on the left hand side of Eq. (32) is negative, and such that the absolute minimum of $R(a)$ is with $a = 0$, even if the derivative of R with respect to a does not vanish for $a \to 0$.

4.2 The Special Case $B \to \infty$

When $B \to \infty$, the third-kind boundary conditions for the temperature become Dirichlet boundary conditions, so that the boundaries at $y = 0, 1$ become in fact perfectly isothermal. In this limit, one has $\eta \to 1$. Thus, for $\lambda_1 \neq 0$ and $\lambda_2 \neq 0$, Eq. (29) is drastically simplified to

$$\sinh \lambda_1 \sinh \lambda_2 = 0, \tag{33}$$

with

$$\lambda_1 = \sqrt{b\left(b + \sqrt{R}\right)}, \quad \lambda_2 = \sqrt{b\left(b - \sqrt{R}\right)}. \tag{34}$$

Since $\sinh \lambda_1 \neq 0$ and $\lambda_2 \neq 0$, Eq. (33) can be satisfied only with $\lambda_2 = im\pi$, where i is the imaginary unit, and m is a positive integer. The condition $\lambda_2 = im\pi$ yields, on account of Eq. (34),

$$R = \frac{(m^2\pi^2 + b^2)^2}{b^2} = \frac{1}{a^2 + \left(\frac{n\pi}{2s}\right)^2}\left[m^2\pi^2 + a^2 + \left(\frac{n\pi}{2s}\right)^2\right]^2,$$
$$n = 0, 1, 2, 3, \ldots, \quad m = 1, 2, 3, \ldots, \tag{35}$$

where we used the definition of the modified wave number given by Eq. (19). Equation (35) is perfectly consistent with the neutral stability condition found, in this special case, by Beck (1972) and recently re-examined in Barletta and Storesletten (2012). From Eq. (35), one may infer that the lowest neutral stability curve in the (b, R)-plane is for $m = 1$, so that the critical values R_c and b_c for the onset of the convective instability are given by

$$R_c = 4\pi^2, \quad b_c = \pi. \tag{36}$$

On account of Eqs. (30)–(32) we conclude that, for a fixed s, we have several values of a_c corresponding to the same b_c, namely

$$a_c = \pi\sqrt{1 - \left(\frac{n}{2s}\right)^2}, \quad n = 0, 1, 2, \ldots, \lfloor 2s \rfloor, \tag{37}$$

where $\lfloor \cdot \rfloor$ denotes the floor function, i.e., the largest integer number less than or equal to its argument. An interesting special case is when the aspect ratio s is an integer or a half-integer, so that we may have $a_c = 0$ for the mode $n = 2s$.

4.3 The Special Case $B \to 0$

Strictly speaking, the limiting case $B \to 0$ describes a rectangular channel where all the four boundary walls are adiabatic. Hence, we have a definitely uninteresting case with respect to the onset of convection, as no basic temperature gradient is supplied to the fluid saturated porous medium. However, one can accomplish the condition $B \to 0$ while keeping the product BR finite. Physically, this means that one approaches the condition $B \to 0$, i.e. $h \to 0$, on gradually increasing the temperature difference ΔT between the lower and the upper fluid environments, so that the product $h\Delta T$ remains finite. Hence, $B \to 0$ means that the third-kind temperature boundary conditions on the horizontal walls are in fact replaced by second-kind temperature boundary conditions. One could well say that, with $B \to 0$, the case of isoflux conditions on the horizontal walls is described (see also Barletta and Storesletten 2012). This special way of intending the limit $B \to 0$ is formulated on defining

$$\tilde{V} = \eta V, \quad \tilde{R} = \eta R. \tag{38}$$

We note that $\tilde{R}$ is a Darcy–Rayleigh number based on the temperature difference between the horizontal boundary walls in the basic state, namely $\eta\Delta T$. Thus, by keeping $\tilde{V} \sim O(1)$ and $\tilde{R} \sim O(1)$, the limit $B \to 0$ of Eqs. (20), (21) and (23) reads

$$\frac{\mathrm{d}^2\tilde{V}}{\mathrm{d}y^2} - b^2\left(\tilde{V} - \tilde{R}G\right) = 0, \tag{39a}$$

$$\frac{\mathrm{d}^2 G}{\mathrm{d}y^2} - b^2 G + \tilde{V} = 0, \tag{39b}$$

$$y = 0, 1 : \quad \tilde{V} = 0, \quad \frac{\mathrm{d}G}{\mathrm{d}y} = 0, \tag{39c}$$

and

$$\lambda_1 = \sqrt{b\left(b + \sqrt{\tilde{R}}\right)}, \quad \lambda_2 = \sqrt{b\left(b - \sqrt{\tilde{R}}\right)}. \tag{40}$$

These equations lead to the neutral stability condition, Eq. (29), where B is set to zero and where λ_1, λ_2 are now given by Eq. (40), namely

$$\frac{\sinh\lambda_1 \sinh\lambda_2}{\lambda_1\lambda_2} - \frac{1 - \cosh\lambda_1 \cosh\lambda_2}{b^2} = 0. \tag{41}$$

A power series expansion of the left hand side of Eq. (41) with respect to b around $b = 0$ yields

$$2 - \frac{\tilde{R}}{6} + \frac{1680 - 112\tilde{R} + \tilde{R}^2}{2520} b^2 + O(b^4) = 0. \tag{42}$$

Equation (42) proves that $\tilde{R} \to 12$ when $b \to 0$, and that $\tilde{R} = 12$ at $b = 0$ is in fact a local minimum of the neutral stability curve $\tilde{R}(b)$. This is a well-known result in the analysis of the isoflux variant to the classical Darcy–Bénard problem (see Sect. 6.2 of Nield and Bejan 2006).

5 Discussion of the Neutral Stability Condition

Plots of the neutral stability curves in the (b, R)-plane are given in Fig. 2. The different plots are relative to different Biot numbers, including the limiting case $B \to \infty$. We note that

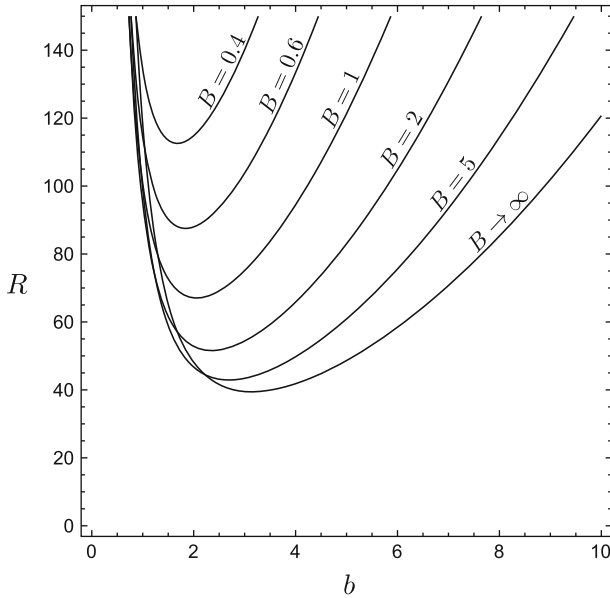**Fig. 2** Neutral stability curves in the (b, R)-plane

the neutral stability curves gradually move upward in the parametric plane as B decreases. This feature is interpreted as the (expected) increased stability of the fluid saturated porous medium when the efficiency of the external convection process diminishes. For a given B, the minimum of the neutral stability curve is at the critical conditions, (b_c, R_c). From Fig. 2, we see that R_c is a decreasing function of B, while b_c is an increasing function of B. This feature is neatly confirmed by Figs. 3 and 4, where the plots of R_c and b_c versus B are displayed, respectively. The asymptotic values of (b_c, R_c) for $B \to \infty$, Eq. (36), are approached monotonically. For very large values of B, accurate correlations for the values of (b_c, R_c) are given by,

$$b_c \cong \pi \left(1 - \frac{1}{B} \right), \quad R_c \cong 4\pi^2 + \frac{166}{B^2}. \tag{43}$$

From the analysis carried out in Sect. 4.3, we can conclude that the asymptotic behaviour of R_c as B approaches zero is

$$R_c \sim \frac{24}{B}, \tag{44}$$

while $b_c \to 0$. In fact, accurate correlations for very small values of B are the following:

$$b_c \cong (\pi - 1)B^{1/4}, \quad \tilde{R}_c \cong 12 + \frac{95}{9} B^{1/2}, \tag{45}$$

where $\tilde{R}_c$ is the critical value of the modified Darcy–Rayleigh number, $\tilde{R}$, defined in Eq. (38). These approximate expressions match the trend of the plots displayed in Figs. 3 and 4. The critical values of b, R, and $\tilde{R}$ are reported in Table 1 spanning the whole range of the possible Biot numbers.

If the neutral stability condition is mapped in the parametric (a, R)-plane, then the dependence on the aspect ratio s of the rectangular duct becomes evident. We have chosen to
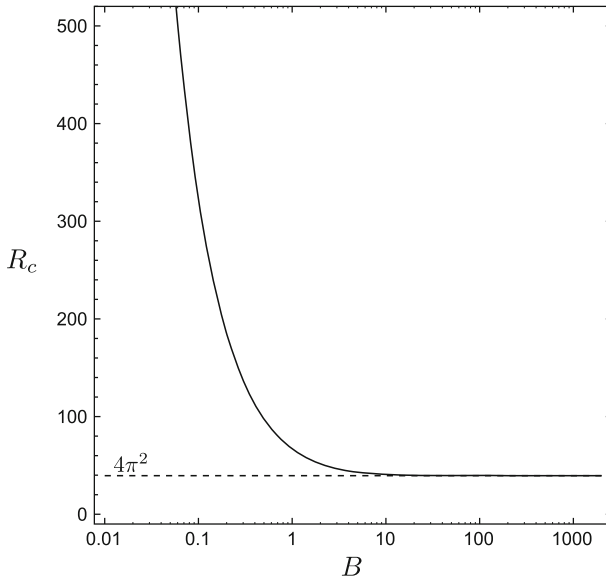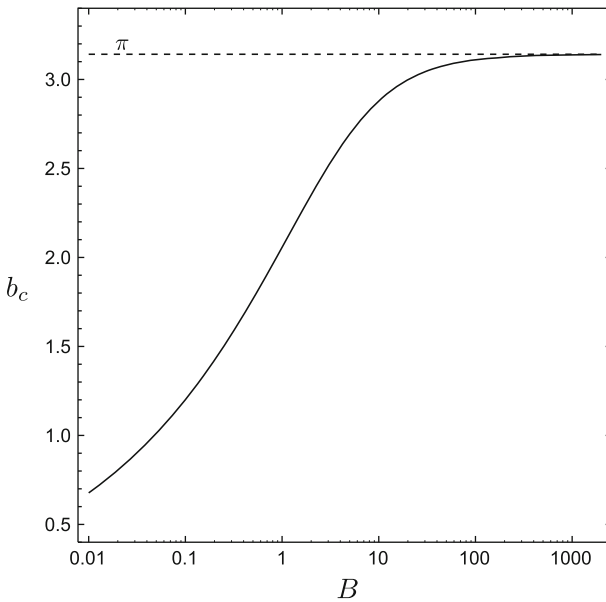
Fig. 3 Critical value R_c versus B

Fig. 4 Critical value b_c versus B

represent the neutral stability condition for three sample cases: a shallow rectangular duct, $s = 1$, a square duct, $s = 1/2$, and a slender rectangular duct, $s = 1/4$. These three cases are illustrated in Figs. 5, 6 and 7. In these figures, the lowest neutral stability curves $R(a)$ are plotted for different Biot numbers. This means that in different ranges of the wave number a, different n-modes provide the lowest neutral stability curve for a given Biot number.

Table 1 Critical values b_c, R_c and $\tilde{R}_c$ for different Biot numbers

B	b_c	R_c	$\tilde{R}_c$
∞	$\pi = 3.14159$	$4\pi^2 = 39.4784$	$4\pi^2 = 39.4784$
2000	3.14002	39.4785	39.4390
1500	3.13950	39.4785	39.4259
1200	3.13898	39.4785	39.4128
1000	3.13846	39.4786	39.3998
500	3.13533	39.4791	39.3218
200	3.12603	39.4826	39.0917
100	3.11075	39.4949	38.7205
50	3.08102	39.5415	38.0207
20	2.99828	39.8252	36.2047
15	2.95616	40.0560	35.3435
12	2.91653	40.3273	34.5663
10	2.87916	40.6322	33.8601
5	2.69303	42.9232	30.6594
2	2.35142	51.5835	25.7917
1.5	2.23040	56.7119	24.3051
1.2	2.13490	61.8836	23.2063
1	2.05666	67.0569	22.3523
0.9	2.01161	70.4974	21.8785
0.8	1.96151	74.7839	21.3668
0.7	1.90521	80.2688	20.8104
0.6	1.84106	87.5329	20.1999
0.5	1.76661	97.6103	19.5221
0.4	1.67795	112.542	18.7570
0.3	1.56817	137.016	17.8716
0.2	1.42291	184.832	16.8029
0.1	1.20120	323.215	15.3912
0.05	1.01181	589.935	14.3887
0.02	0.805277	1363.75	13.5024
0.01	0.677237	2624.79	13.0586
0.005	0.569475	5111.34	12.7465
0.002	0.452845	12483.3	12.4708
0.001	0.380769	24677.2	12.3325
0	0	∞	12

The transition from a n-mode to its successor is accompanied by a cusp point of the lowest neutral stability curve.

In Fig. 5, we consider a shallow rectangular channel ($s = 1$). In the case $B \to \infty$, the modes $n = 0, 1, 2$ yield the lowest neutral stability curve. In particular, the mode $n = 2$ dominates for very low values of a, so that R reaches the critical value $R_c = 4\pi^2$ when $a \to 0$. This conclusion is perfectly consistent with the multiplicity of critical wave numbers, a_c, leading to the same R_c discussed in Sect. 4.2. The multiplicity of critical wave
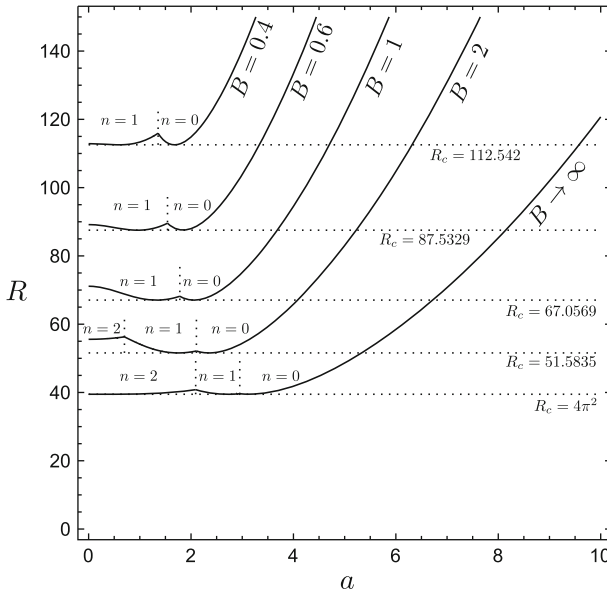
Fig. 5 Lowest neutral stability curves with $s = 1$ in the (a, R)-plane, for different Biot numbers
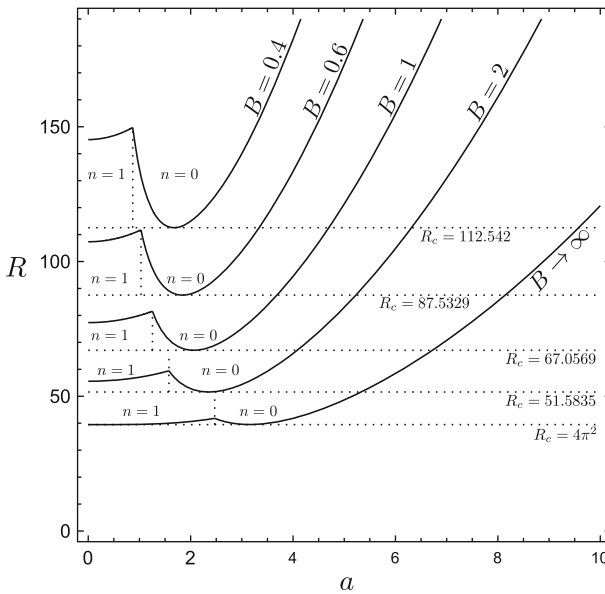

Fig. 6 Lowest neutral stability curves with $s = 1/2$ in the (a, R)-plane, for different Biot numbers

numbers corresponding to the same R_c is displayed in Fig. 5 also for finite Biot numbers, $B = 0.4, 0.6, 1, 2$. The most apparent differences with respect to the case $B \to \infty$ are that the limit $a \to 0$ does not mean in general $R \to R_c$, as it happens for the case $B \to \infty$. Moreover, with a finite B, less n-modes than in the case $B \to \infty$ display their minimum at
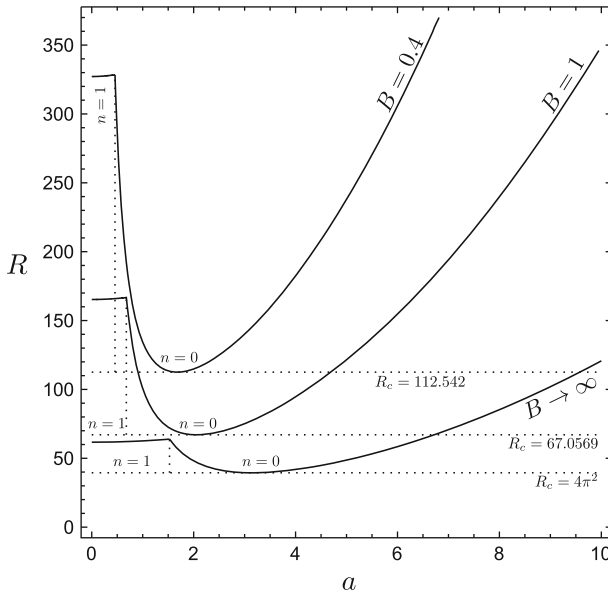
Fig. 7 Lowest neutral stability curves with $s = 1/4$ in the (a, R)-plane, for different Biot numbers

$R = R_c$. This last feature is expected on the basis of Eqs. (30)–(32), if one considers that b_c decreases as B decreases.

The features described with reference to Fig. 5 are basically shared also by Figs. 6 and 7. However, only the modes $n = 0$ and $n = 1$ are involved in these figures, and this is a consequence of the smaller values of the aspect ratio, $s = 1/2$ and $s = 1/4$, respectively. Again, the explanation comes from Eqs. (30)–(32). A peculiar feature of Figs. 6 and 7 is that the transition from the mode $n = 0$ to the mode $n = 1$ takes place for high values of R especially when B is small. The reason here is that the neutral stability value of R with the two-dimensional modes, i.e. with the normal modes having $a = 0$, rapidly increases when s tends to zero. This behaviour of the two-dimensional modes is illustrated in Fig. 8.

The analysis of the two-dimensional modes with $a = 0$ shows that, except for some very special aspect ratios s depending on the assigned Biot numbers, the critical conditions for the onset of convection can be only produced with three-dimensional, z-dependent, normal modes. This conclusion can be drawn on inspecting Fig. 8. We denoted by R_0 the lowest neutral stability value of R in the limit $a \to 0$. We have already noted in Sect. 4.2, with reference to the limit $B \to \infty$, that R_0 coincides with R_c when s is either an integer or a half integer, and this feature is clearly identified in Fig. 8. When B is finite, one may still have $R_0 = R_c$ for special values of s. These values, denoted as s_n, are easily found for given B and n on employing Eq. (30) with $a_c = 0$, namely

$$s_n = \frac{n\pi}{2b_c}, \quad n = 1, 2, 3, \ldots. \tag{46}$$

For instance, if $B = 1$, we find in Table 1 the value $b_c = 2.05666$, so that we obtain from Eq. (46):

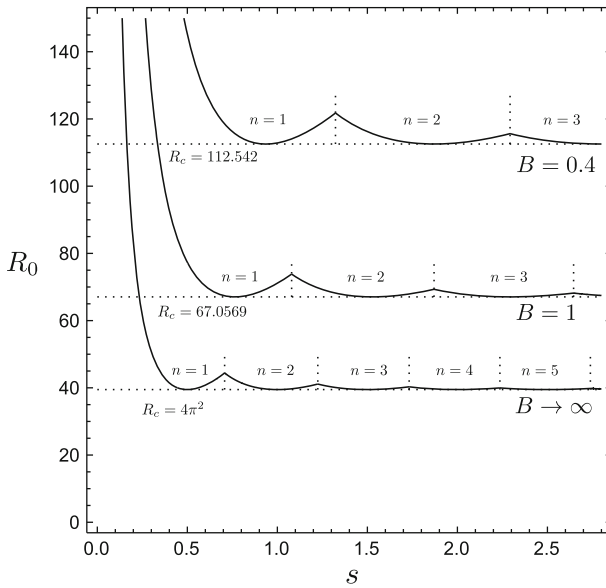$$s_1 = 0.763759, \quad s_2 = 1.52752, \quad s_3 = 2.29128, \quad s_4 = 3.05504, \ldots.$$

Fig. 8 Lowest neutral stability curves, $R_0(s)$, for the two-dimensional modes ($a = 0$), with different Biot numbers

Figure 9 shows the neutral stability curve for the limiting case $B \to 0$ in the $(b, \tilde{R})$-plane. An important fact is that the neutral stability curve defines in this case a monotonic increasing function $\tilde{R}(b)$. As a consequence of Eq. (19), this means that the lowest neutral stability curve in the $(a, \tilde{R})$-plane is with $n = 0$ for every $a > 0$. Equation (19) yields for $n = 0$ the identity $a = b$, so that we have no difference between the representation of the neutral stability curve in the $(b, \tilde{R})$-plane and that in the $(a, \tilde{R})$-plane. Moreover, on account of the conclusions drawn in Sect. 4.3, we now infer that the critical conditions for the onset of convection are $b_c = a_c = 0$ and $\tilde{R}_c = 12$.

6 A Finite Porous Box

Hitherto, we considered the length of the rectangular channel along the z-direction as infinite. We based on this assumption our analysis of Fig. 8, leading us to the conclusion that the onset of convection occurs necessarily through three-dimensional normal modes, except for a discrete sequence of special aspect ratios dependent on the assigned Biot number. This conclusion is reached as a consequence of the hypothesis that the wave number a has a continuous spectrum, and this hypothesis is correct only if the rectangular channel is infinite along the z-direction. Assuming a finite length in the z-direction means that the rectangular channel is in fact a porous box with sides $2L$ (in the x-direction), H (in the y-direction), and D (in the z-direction). This means that we can define a secondary aspect ratio,

$$d = \frac{D}{H}, \tag{47}$$

and that the wave number a cannot be considered as a continuous variable. In fact, if d is the dimensionless box length in the z-direction, it is not restrictive to consider $z \in [0, d]$.
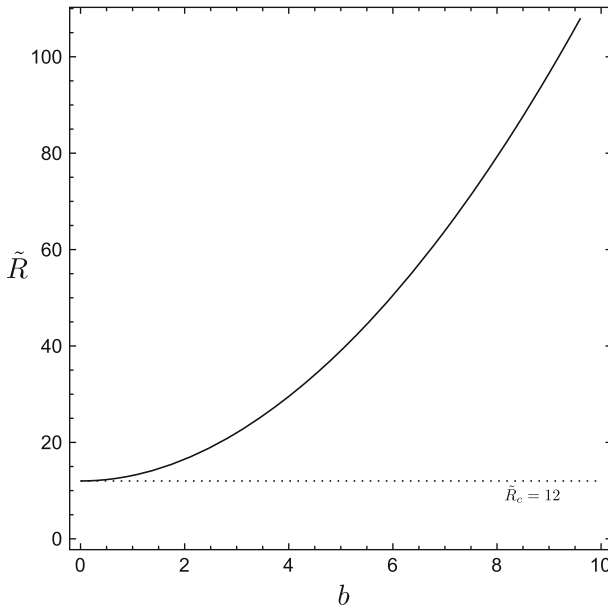
Fig. 9 Neutral stability curve, for the limiting case $B \to 0$, in the $(b, \tilde{R})$-plane

We further assume that the end planes $z = 0$ and $z = d$ are adiabatic and impermeable. Thus, Eq. (13) implies that the wave number a can only assume the discrete values

$$a_\ell = \frac{\ell \pi}{d}, \quad \ell = 0, 1, 2, \ldots, \tag{48}$$

and that the modified wave number b, defined by Eq. (19), assumes discrete values as well,

$$b_{n,\ell} = \sqrt{\left(\frac{n \pi}{2s}\right)^2 + \left(\frac{\ell \pi}{d}\right)^2}, \quad n, \ell = 0, 1, 2, \ldots. \tag{49}$$

We pointed out in Sect. 4.1 that, under conditions of neutral stability, the Darcy–Rayleigh number R depends only on the modified wave number b, once the Biot number B has been prescribed. This means that, for any fixed B, one can seek the (n, ℓ)-mode leading to the lowest neutral stability value of R. Since, at neutral stability, $R = R(b)$ and b is given by Eq. (49), the answer changes with the aspect ratios s and d, and the results may be reported in many ways. Beck (1972) and Wang (1999), as well as Kubitschek and Weidman (2003), chose to report the selected (n, ℓ)-modes at the onset of the convective instability through a two-dimensional (s, d)-diagram, now well-known as Beck's diagram. In this article, we preferred to collect the same information by plotting $R(d)$ for fixed values of s and B. Figures 10, 11 and 12 show these plots for $B = 2$ (Fig. 10), for $B = 1$ (Fig. 11), and for $B = 0.5$ (Fig. 12). Each figure displays the plots of $R(d)$, with $s = 1/4, 1/2, 1, 2$.

Figures 10, 11 and 12 reveal that the modes with $\ell = 0$ define the least stable planform at the onset of convection, provided that the rectangular channel is sufficiently short in the z-direction. As one can infer from Eqs. (13) and (48), the modes with $\ell = 0$ are two-dimensional so that the disturbances are independent of z. From Figs. 10, 11 and 12, one can thus conclude that the onset of convection takes place with $\ell = 0$ modes when d is smaller than a threshold value, while it becomes z-dependent when this threshold is exceeded. The threshold
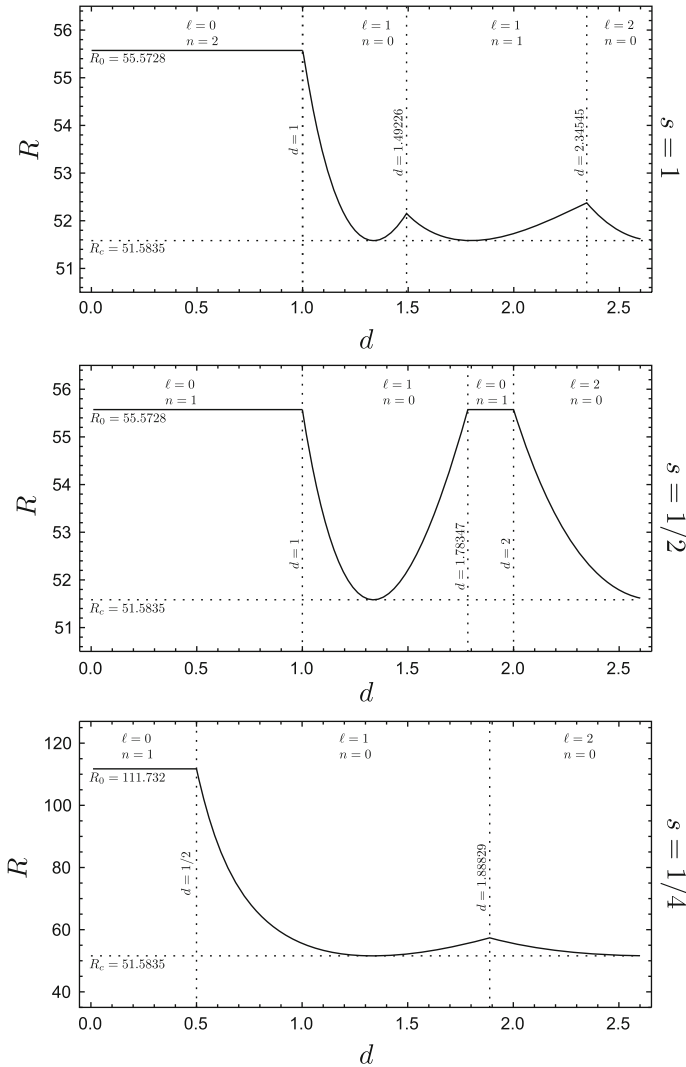
Fig. 10 Neutral stability condition in a finite box: plots of R versus d for $B = 2$

value of d is strongly dependent on the pair of input parameters (s, B). The same holds also for the other values of d that mark the transition from one (n, ℓ)-mode to another (n, ℓ)-mode in defining the least stable condition. Figures 10, 11 and 12 show that the two-dimensional ($\ell = 0$) mode leading to the lowest neutral stability value of R (we denoted this value as R_0) is dependent on the pair (s, B), as we have pointed out when we commented on Fig. 8. We mention that, in some cases, the threshold values separating different (n, ℓ)-modes are rational numbers. The reason is that R is a function of $b = b_{n,\ell}$ and, as evidenced in Eq. (49), the same b can be obtained with different pairs (n, ℓ). For instance, in Fig. 10, the threshold $d = 1$ separating the modes $(n = 2, \ell = 0)$ and $(n = 0, \ell = 1)$ for $s = 1$ can be explained by this simple reasoning. We recall that $R(b)$ at neutral stability is not an injective function, so that the same R can be produced with different values of b. This explains why some transition
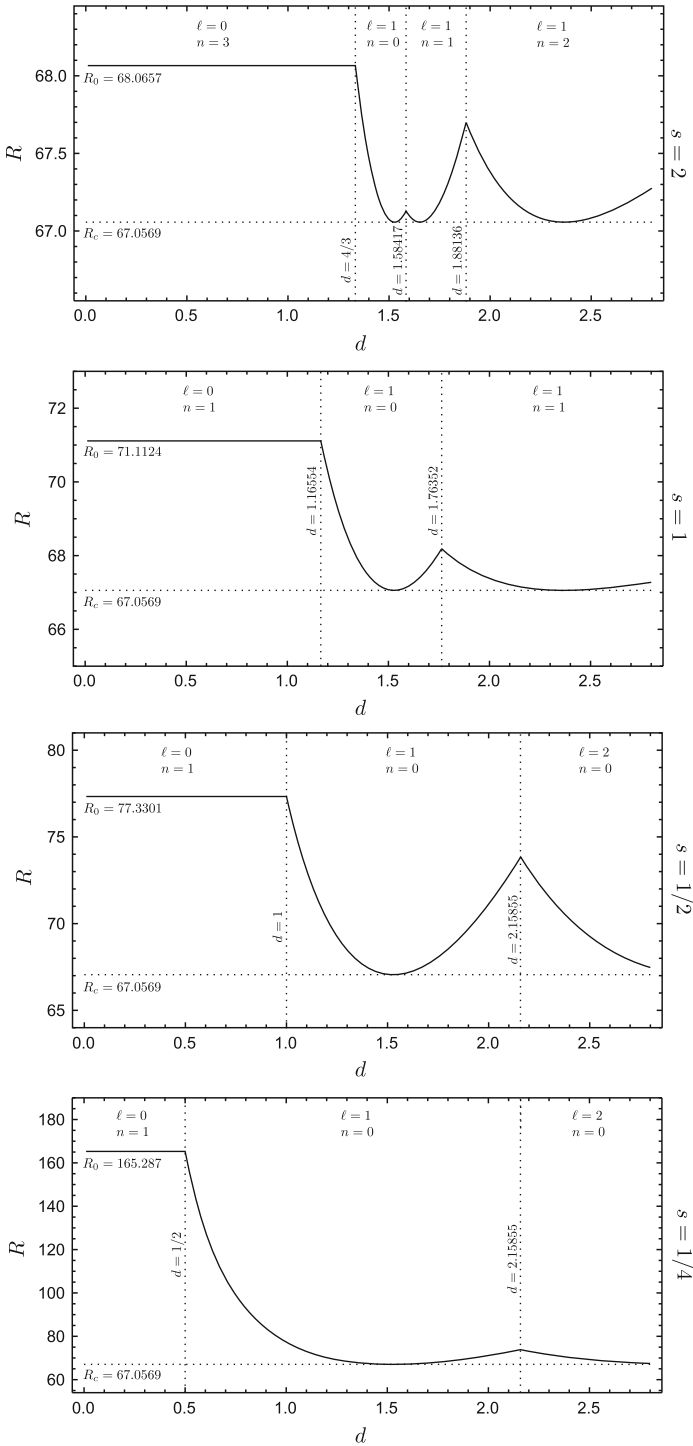
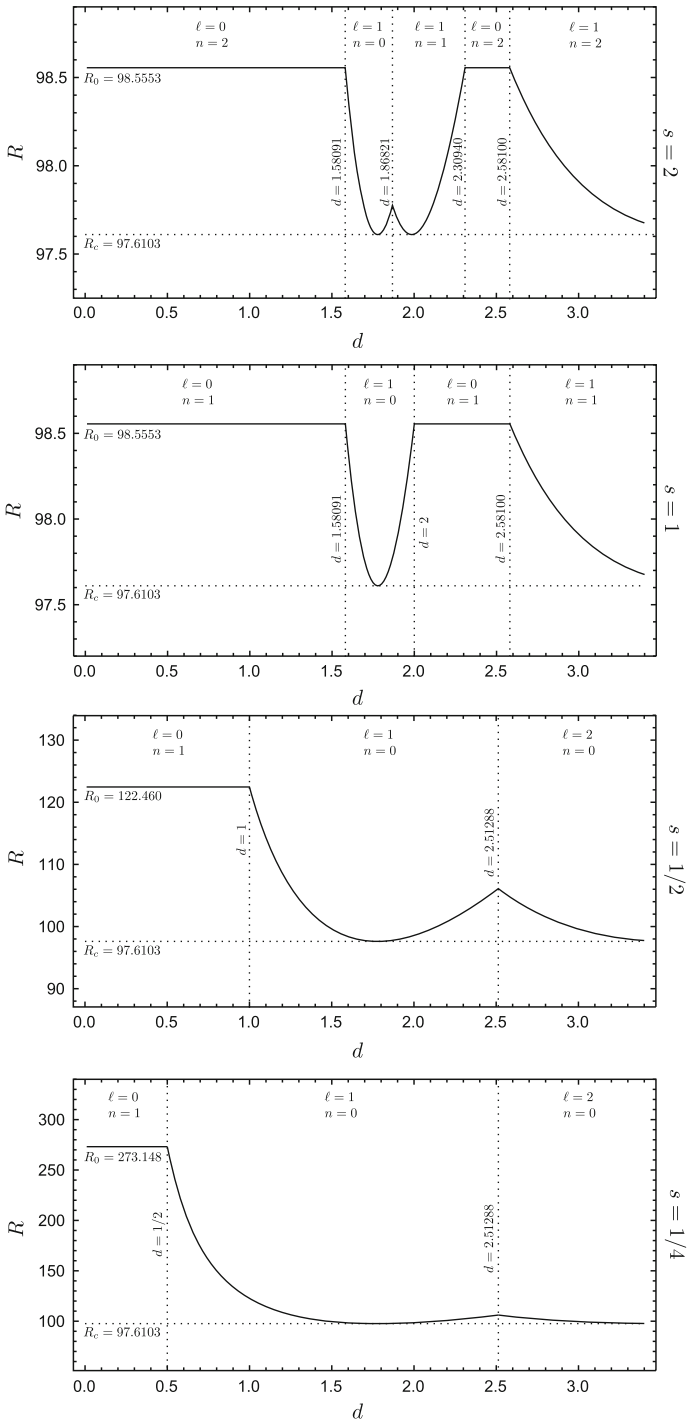**Fig. 11** Neutral stability condition in a finite box: plots of R versus d for $B = 1$

Fig. 12 Neutral stability condition in a finite box: plots of R versus d for $B = 0.5$

values of d displayed in Figs. 10, 11 and 12 are not rational numbers. We report that, with slender rectangular cross-sections ($s = 1/4$), the transition to z-dependent modes at the onset of convection takes place with the smallest threshold value of d, i.e. $d = 1/2$, in all the examined cases: $B = 0.5, 1, 2$. Unlike Figs. 11 and 12, Fig. 10 does not contain the frame relative to $s = 2$. The reason is that, with $B = 2$ and $s = 2$, we have $R_0 - R_c \cong 2 \times 10^{-4}$, with R_0 being given by the mode ($n = 3, \ell = 0$). As a consequence, the plot of R versus d would be compressed in an extremely small vertical range. Since the difference $R_0 - R_c$ is so small, it is practically useless in this case to question whether the mode ($n = 3, \ell = 0$) is more or less stable than the modes with $\ell \neq 0$.

A final remark concerns the limiting cases $B \to \infty$ and $B \to 0$. As pointed out in Sect. 4.2, the value of R_0 coincides with R_c in the limit $B \to \infty$, whenever s is an integer or a half-integer. This means that, with the aspect ratios considered in Figs. 10, 11 and 12, $s = 1/2, 1, 2$, and with $B \to \infty$, the onset of convection may always occur with $\ell = 0$ modes for every value of d. The case $s = 1/4$ is evidently different, and we deduce from Beck's diagram (Beck 1972, relative to the case $B \to \infty$) that the threshold value of d for the transition to z-dependent modes is $d = 1/2$, as in all the cases with a finite B examined in Figs. 10, 11, and 12. The analysis of the limiting case $B \to 0$ is extremely simple. In fact, as pointed out in Sect. 4.3 and illustrated in Fig. 9, the neutral stability function $\tilde{R} = \tilde{R}(b)$ is monotonic increasing when $B \to 0$. This means that the least stable (n, ℓ)-mode at the onset of convection is either the mode ($n = 1, \ell = 0$), or the mode ($n = 0, \ell = 1$), depending on the considered pair of aspect ratios (s, d). The mode ($n = 1, \ell = 0$) is preferred when $d < 2s$, as it can be easily inferred from the monotonicity of the neutral stability function $\tilde{R} = \tilde{R}(b)$, and from Eq. (49).

7 Conclusions

The onset conditions of the thermal instability in a horizontal fluid saturated porous channel with a rectangular cross-section have been studied. A three-dimensional linear stability analysis of the stationary normal mode disturbances of the zero-velocity basic solution has been carried out. In the stability analysis, we have considered thermally insulated and impermeable side walls, and we have assumed that the horizontal boundary walls are impermeable and subject to third-kind temperature conditions. These temperature boundary conditions at the horizontal walls describe an external convection heat transfer to a lower fluid environment at a reference temperature $T_0 + \Delta T$ and to a upper fluid environment at a temperature T_0. When the external heat transfer coefficient tends to infinity, the third-kind temperature boundary conditions become of Dirichlet type, while they become of Neumann type when the heat transfer coefficient tends to zero. In the former limit, the problem investigated in this paper coincides with that studied by Beck (1972).

The governing dimensionless parameters of the linear stability are the width-to-height aspect ratio s of the channel cross-section, the Biot number B associated with the temperature boundary conditions at the horizontal walls, and the Darcy–Rayleigh number R. The latter parameter defines the onset of convection through the neutral stability relationship $R = R(a)$, where a is the dimensionless wave number along the longitudinal z-direction. The neutral stability condition has been determined by solving analytically the linearised disturbance equations. The main features of the stability analysis are outlined in the following.

- Compared to the limiting case $B \to \infty$, originally investigated by Beck (1972), the onset conditions of the instability for a finite Biot number imply higher values of the critical Darcy–Rayleigh number R_c. More precisely, R_c increases as B decreases.
- The limiting case $B \to 0$ has been studied by employing a rescaling of the parameter R, so that this limiting case is relative to a rectangular channel with isoflux horizontal walls. In this limit, the critical Darcy–Rayleigh number R_c is equal to 12 and, thus, it coincides with the well-known result obtained for a horizontal porous layer ($s \to \infty$) with isoflux boundaries (see Sect. 6.2 of Nield and Bejan 2006).
- By changing the aspect ratio s, for a given Biot number, we found that the neutral stability curve $R(a)$ changes. On the other hand, the critical values of the Darcy–Rayleigh number were shown to be independent of s. In particular, several critical wave numbers a_c corresponding to the same critical Darcy–Rayleigh number R_c are displayed for a given pair (s, B). The multiplicity of the allowed values of a_c sensibly depends on s and on B.
- We considered the case of a rectangular channel with a finite length in the longitudinal z-direction, i.e. a finite porous box. We studied the effect of the length-to-height aspect ratio d on the neutral stability condition. The main result is that the preferred modes of instability are independent of the z-coordinate only when the value of d is sufficiently small, the threshold value being dependent on the Biot number B and on the width-to-height aspect ratio s. This means that a two-dimensional analysis of the instability, in the (x, y)-plane of the channel cross section, allows the detection of the least stable normal modes only if the rectangular channel is sufficiently short.

References

Barletta, A: Thermal instabilities in a fluid saturated porous medium. In: Öchsner, A., Murch, G.E. (eds.) Heat Transfer in Multi-Phase Materials, pp. 381–414. Springer, New York (2011)

Barletta, A., Celli, M., Kuznetsov, A.V.: Transverse heterogeneity effects in the dissipation-induced instability of a horizontal porous layer. ASME J. Heat Transf. **133**, 122601 (2011)

Barletta, A., Celli, M., Kuznetsov, A.V.: Heterogeneity and onset of instability in Darcy's flow with a prescribed horizontal temperature gradient. ASME J. Heat Transf. **134**, 042602 (2012)

Barletta, A., Storesletten, L.: Onset of convective rolls in a circular porous duct with external heat transfer to a thermally stratified environment. Int. J. Therm. Sci. **50**, 1374–1384 (2011)

Barletta, A., Storesletten, L.: A three-dimensional study of the onset of convection in a horizontal, rectangular porous channel heated from below. Int. J. Therm. Sci. **55**, 1–15 (2012)

Beck, J.L.: Convection in a box of porous material saturated with fluid. Phys. Fluids **15**, 1377–1383 (1972)

Incropera, F.P., Bergman, T.L., Lavine, A.S., DeWitt, D.P. : Fundamentals of Heat and Mass Transfer. 7th edn. Wiley, New York (2011)

Kubitschek, J.P., Weidman, P.D.: Stability of a fluid-saturated porous medium heated from below by forced convection. Int. J. Heat Mass Transf. **46**, 3697–3705 (2003)

Mojtabi, A., Rees, D.A.S.: The effect of conducting bounding plates on the onset of Horton-Rogers-Lapwood convection. Int. J. Heat Mass Transf. **54**, 293–301 (2011)

Nield, D.A.: Onset of thermohaline convection in a porous medium. Water Resour. Res. **4**, 553–560 (1968)

Nield, D.A., Bejan, A.: Convection in Porous Media. 3rd edn. Springer, New York (2006)

Nygård, H.S., Tyvand, P.A.: Onset of convection in a porous box with partly conducting and partly penetrative sidewalls. Transp. Porous Media **84**, 55–73 (2010)

Nygård, H.S., Tyvand, P.A.: Onset of thermal convection in a vertical porous cylinder with a partly conducting and partly penetrative cylinder wall. Transp. Porous Media **86**, 229–241 (2011)

Rees, D.A.S: The stability of Darcy–Bénard convection. In: Vafai, K., Hadim, H.A. (eds.) Handbook of Porous Media, Chapter 12, pp. 521–558. CRC Press, New York (2000)

Rees, D.A.S., Mojtabi, A.: The effect of conducting boundaries on weakly nonlinear Darcy–Bénard convection. Transp. Porous Media **88**, 45–63 (2011)

Ribando, R.J., Torrance, K.E.: Natural convection in a porous medium: Effects of confinement, variable permeability, and thermal boundary conditions. ASME J. Heat Transf. **98**, 42–48 (1976)

Tyvand, P.A.: Onset of Rayleigh–Bénard convection in porous bodies. In: Ingham, D.B., Pop, I. (eds.) Transport Phenomena in Porous Media II, Chapter 4, pp. 82–112. Pergamon, New York (2002)

Wang, C.Y.: Onset of convection in a fluid-saturated rectangular box, bottom heated by constant flux. Phys. Fluids **11**, 1673–1675 (1999)

Weidman, P.D., Kassoy, D.R.: The influence of side wall heat transfer on convection in a confined saturated porous medium. Phys. Fluids **29**, 349–355 (1986)